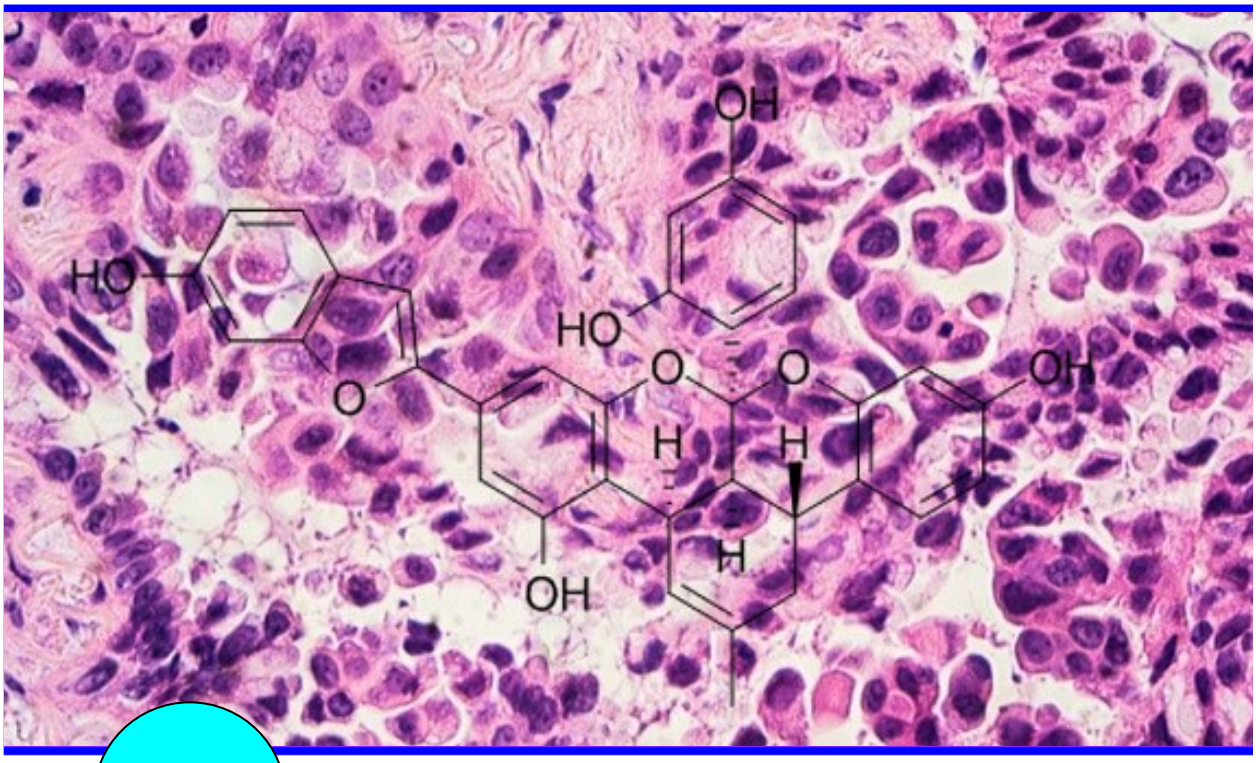

BJP

Bangladesh Journal of Pharmacology

Research Article

Mulberrofuran G inhibits proliferation and migration by inactivating JAK2/STAT3 signaling in lung cancer

A Journal of the Bangladesh Pharmacological Society (BDPS)
Journal homepage: www.banglajol.info; www.bdpsjournal.org
Abstracted/indexed in Academic Search Complete, Agroforestry Abstracts, Asia Journals Online, Bangladesh Journals Online, Biological Abstracts, BIOSIS Previews, CAB Abstracts, Current Abstracts, Directory of Open Access Journals, EMBASE/Excerpta Medica, Global Health, Google Scholar, HINARI (WHO), International Pharmaceutical Abstracts, Open J-gate, Science Citation Index Expanded, SCOPUS and Social Sciences Citation Index
Bangladesh J Pharmacol 2021; 16: 134-140
ISSN: 1991-0088

Mulberrofuran G inhibits proliferation and migration by inactivating JAK2/STAT3 signaling in lung cancer cells

Hai-Yuan-Bo Guo[1], Xiao-Xiao Liu[2], Xiao-Yong Zhu[3] and Zhe Yu[4]

[1]Department of Medical Oncology, Pinghu Second People's Hospital, Pinghu City, Zhejiang Province 314200, China; [2]Department of Medical Oncology, Xinchang People's Hospital of Zhejiang Province, Shaoxing City, Zhejiang Province 312500, China; [3]Department of Second Ward of Medical Oncology, Zhuji People's Hospital of Zhejiang Province, Shaoxing City, Zhejiang Province 311800, China; [4]Department of Respiratory Medicine, HwaMei Hospital, University of Chinese Academy of Sciences, Ningbo City, Zhejiang Province 315099, China.

Article Info

Received: 17 August 2021
Accepted: 20 December 2021
Available Online: 26 December 2021

DOI: 10.3329/bjp.v16i4.55198

Cite this article:
Guo HYB, Liu XX, Zhu XY, Yu Z. Mulberrofuran G inhibits proliferation and migration by inactivating JAK2/STAT3 signaling in lung cancer cells. Bangladesh J Pharmacol. 2021;

Abstract

The present study has investigated how mulberrofuran G affects proliferation, invasion, and migration of the lung adenocarcinoma and squamous cell carcinoma. Four different concentrations of mulberrofuran G (1, 5, 10, and 100 µmol/L) were used to simulate human lung adenocarcinoma cells (A549 cells) and squamous-cell carcinoma (NCI-H226 cells). The results showed that mulberrofuran G significantly inhibited the proliferation, invasion, and migration of both A549 and NCI-H226 cells, with a dose-effect relationship. The IC_{50} inhibited the growth of A549 cells and NCI-H226 cells by mulberrofuran G were 22.5 and 30.6 µmol/L, respectively. It strengthened the expression of CDK4 and MMP9 but significantly weakened the expression of p27 in both A549 cells and NCI-H226 cells. Furthermore, the expression of p-JAK2 and p-STAT3 was significantly down-regulated in drug treatments. In conclusion, mulberrofuran G could inhibit proliferation, migration, and invasion of lung cancer cells via inactivating JAK2/STAT3 signaling.

Introduction

Lung cancer is the leading cause of cancer mortality, with estimating 2.1 million new diagnosed cases (approximately 11.6% of all types of cancer cases) and 1.8 million deaths (about 18.4% of all types of cancer deaths) (Bray et al., 2018). Non-small cell lung cancer (NSCLC) and small cell lung cancer (SCLC) are two types of lung cancer. Among the NSCLC, adenocarcinoma of the lung and squamous cell carcinoma of the lung are two major subtypes.

Chemotherapy is the most common method of lung cancer treatment. Despite this, poor prognosis and drug resistance are still inescapable, especially in patients with advanced lung cancer. It is well-known that poor clinic outcome of the solid malignant tumor is attributable to cancer invasion and metastasis (Gupta and Massagué, 2006). Hence, a comprehensive assessment of how to distinguish the key molecular and genetic pathways and how the pathways work in the invasion and metastasis of cancer is a pressing issue.

The JAK/STAT signaling pathway is comprised of Janus kinases (JAKs), signal transducer and activator of transcription proteins (STATs) and binding receptor (Aaronson and Horvath, 2002). The pathway mediates signals transferring from outside to nucleus of a cell. Many studies have investigated the potential roles of JAK/STAT signaling pathway in lung cancer, hematopoietic cancer, primary mediastinal large B-cell lymphoma, and breast cancer (Haque et al., 2018; Fortschegger et al., 2021; Li et al., 2021; Szydłowski et al., 2021).

Mulberrofuran G is isolated from the bark of *Morus alba* (Li et al., 2018). A recent study has indicated that mul-

berrofuran G has a neuroprotective effect in cerebral ischemia through suppressing NOX4 protein expression and NOX4-induced reactive oxygen species (ROS) generation and endoplasmic reticulum stress (Hong et al., 2017). However, elevated NOX4 activity is associated with drug resistance in cancer (Shanmugasundaram et al., 2017). Moreover, mulberrofuran G is dual inhibitor of protein tyrosine phosphatase 1B (PTP1B) and α-glucosidase enzymes (Paudel et al., 2018). The deficiency or inhibition of PTP1B mediates the metastasis process in lung cancer (Chen et al., 2020). However, this knowledge gap is of considerable concern given the effect of mulberrofuran G on lung cancer.

Therefore, the study aimed to illustrate how mulberrofuran G impacts the proliferation, invasion, and migration of lung cancer cells and to evaluate the hypothesis of whether or not mulberrofuran G regulated these processes via the JAK2/STAT3 signaling pathway.

Materials and Methods

Preparation of mulberrofuran G solution

Mulberrofuran G (CAS 87085-00-5, HPLC≥98%) was purchased from Shanghai Tauto Biotech Co., Ltd. and dissolved in phosphate-buffered saline to make the solutions with 4 final concentrations of 1, 5, 10, and 100 μmol/L.

Cell lines and cell culture

The human lung adenocarcinoma cell line (A549 cells) and human lung squamous cell carcinoma cell line (NCI-H226 cells) were purchased from the Cell Bank of Type Culture Collection of The Chinese Academy of Sciences (China). A549 cells and NCI-H226 cells were cultured in Roswell Park Memorial Institute 1640 (RPMI-1640, Thermo Fisher Scientific) medium containing 10% fetal bovine serum (Thermo Fisher Scientific) at 37°C in a humidified air containing 5% CO_2 incubator (Thermo Fisher Scientific). Cell passage was carried out by the usual procedure and the third generation cells were used for the subsequent experiments.

CCK8 assay

A549 cells (1×10^4 cells/well) and NCI-H226 cells (1×10^4 cells/well) in the logarithmic growth phase were seeded into 96-well plates and permitted to adhere overnight, respectively. The cells were then administrated with 100 μL 1, 5, 10 and 100 μmol/L mulberrofuran G. The control group was treated with an equal volume of phosphate-buffered saline. After treatment for 24 hours, 100 μL of medium containing 10% cck8 was replaced, and continuously cultured for 2 hours at 37°C in a humidified air containing 5% CO_2. The optical density at 450 nm was measured by a microplate reader (PT-3502PC) and used as the positive index of cell viability.

Cell colony assay

A549 cells and NCI-H226 cells (approximately 2×10^3 cells) were suspended in 1, 5, 10 and 100 μmol/L mulberrofuran G containing 0.33% agar, RPMI 1640 medium, 10% fetal bovine serum, respectively. Thereafter, the mixture containing 0.5% agar, RPMI 1640 medium, and 10% fetal bovine serum were administrated in an upper layer with a 6-well plate. Followed by an incubation period of 10 days, the colonies of cells (>0.1 mm in diameter) were counted and photographed by an inverted microscope. Each treatment had three replicates and was repeated three times.

Scratch assay

A549 cells and NCI-H226 cells were seeded into 6-well plates, respectively. After incubated for 6 hours at 37°C, 1, 5, 10 and 100 μmol/L mulberrofuran G were used to treat the adhered cells. When the confluence rate of cells

Box 1: Transwell Invasion Assay

Principle

The most characteristic readout of a migration assay is the change of the cell-covered area (gap closure) over time. The cells should be monitored immediately after the gap creation, in most cases by using phase contrast microscopy at different time points (e.g., after 6 and 12 hours).

Requirements

Crystal violet, Fetal bovine serum (10%), Incubator with 5% CO_2, Human lung adenocarcinoma cell line (A549 cells) suspensions (1×10^5 cells), Human lung squamous cell carcinoma cell line (NCI-H226 cells) suspensions (1×10^5 cells), RPMI 1640 medium, Mulberrofuran G, Paraformaldehyde, Phase contrast microscopy Phosphate-buffered saline, Transwell chamber

Procedure

Step 1: 0.1 mL cell suspensions containing 1, 5, 10, and 100 μmol/L mulberrofuran G were seeded into the Transwell chamber.

Step 2: Then, 0.6 mL of RPMI 1640 medium containing fetal bovine serum was added to the lower chamber.

Step 3: All chambers were incubated for 24 hours at 37°C in a humidified air containing 5% CO_2.

Step 4: Cells in the lower chamber were fixed with 4% paraformaldehyde for 10 min after removing the Transwell chamber.

Step 5: The cells were stained with crystal violet for 25 min, washed with phosphate-buffered saline, placed under phase contrast microscopy and photographed five random fields. Each treatment was repeated three times.

Reference

Pijuan et al., 2019

Reference (video)

Chen, 2018

reached 95% or more, using a p200 pipette tip generated the "scratch" by scraping the monolayer in a neat and straight line (Liang et al., 2007). The plate was then washed with phosphate-buffered saline. Fresh RPMI 1640 medium containing 10% fetal blood serum was added and cultured at 37°C in a humidified air containing 5% CO_2. The plates were examined at 0 and 24 hours after being scratched. The ability of migration was evaluated by the formula: wound closure = (Pair $distance_{0hour}$ − Pair dis-$tance_{24hour}$) /Pair $distance_{0hour}$.

Western blot

After administrating A549 cells with 22.5 μmol/L mulberrofuran G and administrating NCI-H226 cells with 30.6 μmol/L mulberrofuran G for 24 hours, the cells were collected and lysed in RIPA buffer for 30 min. The protein samples were collected by low-temperature centrifugation. The concentration of each protein sample was then determined by the BCA method. After 10% SDS-PAGE electrophoresis separation, the gel was transferred to nitrocellulose membranes, blocked with 5% skim milk and probed with a primary antibody (ABCAM) at 4°C overnight (Mahmood and Yang, 2012; Pyo et al, 2019). After washing with TBST, this was followed by probing with the HRP-labeled secondary antibody (ABCAM) for 1 hour at room temperature. The band intensity was then analyzed by an automatic chemiluminescence fluorescence image analysis system (Tanon 5200 Multi) and *Image J* software. The markers of cell cycle included p27, CDK4, CDK6, RB1; the MMP9 was used as the marker of metastasis. β-actin was used as an internal control.

Statistical Analysis

All treatments were carried out in triplicates. All values were expressed as mean ± standard deviation (SD). Statistical analysis was performed using SPSS v20.0 software. The comparison between the two sample means was evaluated by *t* test. The comparison between the treatment and the control was performed by one-way ANOVA. The pairwise comparisons between groups were carried out by the least significant difference method.

Results

Proliferation of lung cancer cells

To evaluate the effect of mulberrofuran G on the proliferation of lung cancer cells, A549 cells and NCI-H226 cells were administrated with various concentrations of mulberrofuran G for 24 hours. CCK8 assay results (Figure 1A) indicated that mulberrofuran G significantly inhibited the proliferation of lung cancer cells ($p<0.05$), with a positive dose-inhibition relationship. The IC_{50} of growth inhibition of A549 cells and NCI-H226 cells were 22.5 μmol/L and 30.6 μmol/L, respectively. The two inhibitory concentrations were used in subsequent experiments. Compared with the control, with increased mulberrofuran G, the number of A549 cells and NCI-H226 cells clones were significantly decreased ($p<0.05$, Figure 1B). No difference in both response variables was detected between A549 cells and NCI-H226 cells. Consequently, it may point out that the mulberrofuran G obviously suppressed the proliferation of lung adenocarcinoma and lung squamous cell carcinoma cells.

Invasion and migration of lung cancer cells

To evaluate the effect of mulberrofuran G on the invasion and migration of A549 cells and NCI-H226 cells, the Transwell invasion assay and scratch assay were performed. Results (Figure 2A) indicated that the number of invasive A549 cells and NCI-H226 cells was significantly inhibited compared with normal control. With increased mulberrofuran G concentration, the number of invasive cells showed a decreasing trend. The scratch assay results showed that the cell migration rate of A549 cells and NCI-H226 was significantly weakened by mulberrofuran G (Figure 2B), with a negative linear relationship. No difference in both response variables was detected between A549 cells and NCI-H226 cells. Consequently, it may point out that mulberrofuran G inhibited the invasion and migration of lung adenocarcinoma and lung squamous cell carcinoma cells.

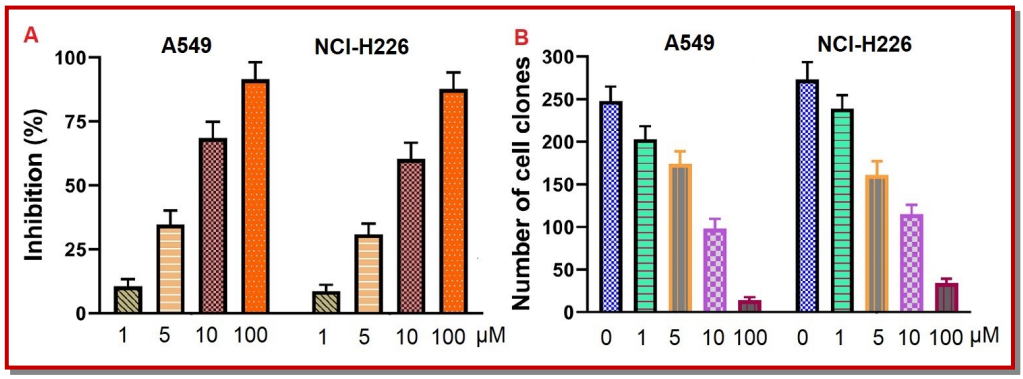

Figure 1: Effects of mulberrofuran G on the proliferation of A549 cells and NCI-H226 cells. (A) CCK8 assay; (B) Cell colony assay

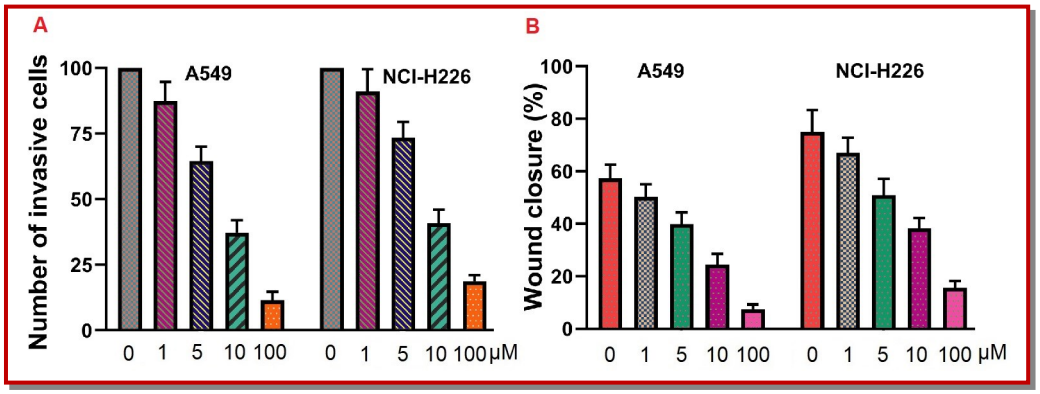

Figure 2: Effects of mulberrofuran G on the invasion and migration of A549 cells and NCI-H226 cells. (A) Transwell invasion assay; (B) Scratch assay

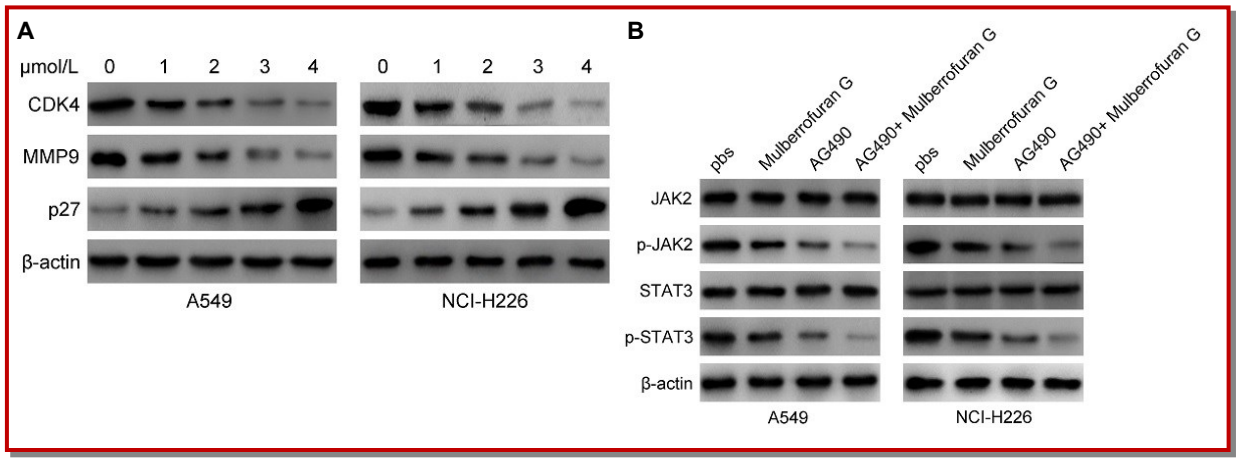

Figure 3: Effects of mulberrofuran G on related markers of the cell cycle (A) and metastasis (B) in A549 cells and NCI-H226 cells. β-actin was used as an internal control (A); Mulberrofuran G inactivated the JAK2/STAT3 signaling pathway in A549 cells and NCI-H226 cells. β-actin was used as an internal control

Cell cycle and metastasis of lung cancer cells

Next, Western blot analysis was performed to evaluate the expression levels of related markers of cell cycle and metastasis. For both A549 cells and NCI-H226 cells, mulberrofuran G significantly down-regulated the expression levels of CDK6 and CDK4, whereas significantly up-regulated the expression levels of p27 and RB1. Further, mulberrofuran G significantly weakened the metastasis-related marker MMP9 in A549 cells (Figure 3A).

JAK2/STAT3 signaling pathway

To illuminate how mulberrofuran G impacted cell proliferation, invasion and migration, A549 cells and NCI-H226 cells were administrated by 22.525 μmol/L and 30.591 μmol/L MG, respectively. The expression levels of JAK2/STAT3 signaling markers were then investigated by a Western blot (Figure 3B). After treatment for 24 hours, there was no difference in JAK2 and STAT3. However, the levels of p-JAK2 and p-STAT3 in A549 cells and NCI-H226 cells were significantly lower than that in the control group ($p<0.05$), which was similar to the effect of JAK2/STAT3 inhibitor AG490. When cells were co-treated with both JAK2/STAT3 inhibitor AG490 and mulberrofuran G, the levels of p-JAK2 and p-STAT3 were the lowest. All the results suggested that mulberrofuran G regulated the proliferation, invasion, and migration of lung cancer cells via inactivating JAK2/STAT3 signaling pathway.

Discussion

Due to the highly invasive and metastatic capacity of tumor cells, the overall survival time of patients with lung cancer is poor; especially patients aged ≥ 75 years (Heist et al., 2017; Cerfolio et al., 2018; Driessen et al., 2018). Better understanding the invasion and migration of tumor cells is the main event prolonging the survival time of individuals with cancer. The present study focuses on the effect of mulberrofuran G on cells proliferation, invasion, and migration of lung adenocarcinoma and squamous cell carcinoma. Previous literature has illuminated that mulberrofuran G plays crucial regulatory roles in several cellular processes (e.g.,

signaling regulation in ROS and protein tyrosine phosphatase) (Hong et al., 2017; Paudel et al., 2018). The proliferations of lung adenocarcinoma and lung squamous cell carcinoma cells were significantly linearly suppressed by mulberrofuran G. By increasing mulberrofuran G, the growth of lung adenocarcinoma and lung squamous cell carcinoma cells were increasingly down-regulated. A recent study has suggested that mulberrofuran G has variable activities, such as anti-Alzheimer's disease, anti-inflammatory, fungicidal, anti -cancer, antibacterial, and anti-tyrosinase properties (Koirala et al., 2018). Hence, this study points to experimental evidence that mulberrofuran G has anti-cancer activity, which provides new insight into the clinical treatment of lung cancer.

Next, the expression level of cell cycle markers was evaluated after treated with various concentrations of mulberrofuran G. Mulberrofuran G prominently weakened the expression levels of CDK6 and CDK4, but strengthened the expression levels of p27 and RB1. At its essence, dysregulation in the cell cycle (e.g. G2/M phase) is associated with the occurrence and development of lung cancer (Ramalingam et al., 2017). The inhibitor p27 regulates the activity of cyclin-dependent kinases (including CDK4 and CDK2); dual Inhibition of CDK4 and CDK2 further induces down-regulation of tyrosine phosphorylation of p27Kip1 (CDKN1B) (Patel et al., 2018). CDK4 and CDK6 inactivate phosphorylations of the central cell cycle/tumor suppressor Rb to initiate G1 phase (Sherr, 1995; Bartek et al., 1996). Degradation of p27Kip1 inhibits cell cycle transition at G1/S boundary and decreases tumor growth (Singh et al., 2018). The deregulation of CDK4 in cancer decreases emerging of E2F-dependent transcription of cyclin E and influences DNA synthesis (Colleoni et al., 2017). Consequently, the proliferation of lung cancer cells is attributable to the p27-mediated down-regulation of CDK4/6 complexes.

Tumor metastasis is the leading cause of mortality in individuals with cancer. The effect of mulberrofuran G on the metastasis of A549 cells and NCI-H226 cells was evaluated. Transwell invasion assay and scratch assay indicated that mulberrofuran G inhibited the invasion and migration of lung adenocarcinoma and lung squamous cell carcinoma cells, with a negatively linear dose-effect relationship. Western blot analysis showed mulberrofuran G significantly down-regulated MMP9 in A549 cells. The regulator MMP-9 plays an important role in the metastasis of cancer cells (Vandooren et al., 2013). Accumulating evidence indicates that up-regulation of MMP9 enhances migration and invasion of cancer cells (Khan et al., 2017; Zhang et al., 2017). The present results suggested that the metastasis of lung cancer cells is linked to inhibition of MMP9 mediated by mulberrofuran G.

Notably, it has been reported that the JAK2/STAT3 signaling pathway is associated with inflammatory response (Weng et al., 2017) and regulated the expression levels of interleukin 6 (IL-6) and MMP-10 in a human lung adenocarcinoma cell (Zhang et al., 2009). The present study showed that mulberrofuran G significantly down-regulated p-JAK2 and p-STAT3 in A549 cells and NCI-H226 cells, which is similar to the effect of JAK2/STAT3 inhibitor AG490. The JAK2/STAT3-specific inhibitor AG490 blocked STAT3 phosphorylation (Liu et al., 2014). The cell growth and migration mediated by JAK2/STAT3 signaling pathway in NSCLC have been reported in several cancers (Liu et al., 2018; Sun et al., 2018). STAT3 is a negative regulator of inflammation (Welte et al., 2003). The activation of STAT3 further enhances the TGF-β/Smad signaling (Zhang et al., 2009) and suppresses p53 transcription (Niu et al., 2005). Mulberrofuran G may have a similar function to AG490. JAK2/STAT3 signaling pathway has protective effects of epidermal growth factor (EGF) receptor activation (Tang et al., 2018). JAK/STAT3 pathway is required to sustain EGF/EGFR-induced epithelial-mesenchymal transition in cancer (Colomiere et al., 2009; Liu et al., 2014). JAK2/ STAT3 pathway is required to strengthen the anti-angiogenic property of anlotinib (Liang et al., 2019).

Conclusion

The anti-cancer effect of mulberrofuran G via inhibition of JAK2/STAT3 signaling pathway to regulate the proliferation, invasion, and migration of lung adenocarcinoma and lung squamous carcinoma cells.

Financial Support

Self-funded

Conflict of Interest

Authors declare no conflict of interest

References

Aaronson DS, Horvath CM. A road map for those who don't know JAK-STAT. Science 2002; 296: 1653-55.

Bartek J, Bartkova J, Lukas J. The retinoblastoma protein pathway and the restriction point. Curr Opin Cell Biol. 1996; 8: 805-14.

Bray F, Ferlay J, Soerjomataram I, Siegel RL, Torre LA, Jemal A. Global cancer statistics 2018: GLOBOCAN estimates of incidence and mortality worldwide for 36 cancers in 185 countries. CA Cancer J Clin. 2018; 68: 394-424.

Cerfolio RJ, Ghanim AF, Dylewski M, Veronesi G, Spaggiari L, Park BJ. The long-term survival of robotic lobectomy for non

–small cell lung cancer: A multi-institutional study. J Thorac Cardiovasc Surg. 2018; 155: 778-86.

Chen Y, Tang J, Lu T, Liu F. CAPN1 promotes malignant behavior and erlotinib resistance mediated by phosphorylation of c-Met and PIK3R2 via degrading PTPN1 in lung adenocarcinoma. Thorac Cancer. 2020; 11: 1848-60.

Chen XL. Lycorine inhibits MDA-MB-231 breast cancer cells proliferation, migration and invasion is associated with Wnt/β-catenin signaling. Bangladesh J Pharmacol. 2018; 13: 192-95.

Colleoni B, Paternot S, Pita JM, Bisteau X, Coulonval K, Davis RJ, Raspé E, Roger PP. JNKs function as CDK4-activating kinases by phosphorylating CDK4 and p21. Oncogene 2017; 36: 4349.

Colomiere M, Ward A, Riley C, Trenerry M, Cameron-Smith D, Findlay J, Ackland L, Ahmed N. Cross talk of signals between EGFR and IL-6R through JAK2/STAT3 mediate epithelial–mesenchymal transition in ovarian carcinomas. Br J Cancer. 2009; 100: 134.

Driessen EJ, Schulkes KJ, Dingemans A-MC, van Loon JG, Hamaker ME, Aarts MJ, Janssen-Heijnen ML. Patterns of treatment and survival among older patients with stage III non-small cell lung cancer. Lung Cancer. 2018; 116: 55-61.

Fortschegger K, Husa AM, Schinnerl D, Nebral K, Strehl S. Expression of RUNX1-JAK2 in human induced pluripotent stem cell-derived hematopoietic cells activates the JAK-STAT and MYC pathways. Int J Mol Sci. 2021; 22: 7576.

Gupta GP, Massagué J. Cancer metastasis: Building a framework. Cell 2006; 127: 679-95.

Haque I, Ghosh A, Acup S, Banerjee S, Dhar K, Ray A, Sarkar S, Kambhampati S, Banerjee SK. Leptin-induced ER-α-positive breast cancer cell viability and migration is mediated by suppressing CCN5-signaling via activating JAK/AKT/STAT-pathway. BMC Cancer. 2018; 18: 99.

Heist RS, Guarino MJ, Masters G, Purcell WT, Starodub AN, Horn L, Scheff RJ, Bardia A, Messersmith WA, Berlin J. Therapy of advanced non–small-cell lung cancer with an SN-38-anti-trop-2 drug conjugate, sacituzumab govitecan. J Clin Oncol. 2017; 35: 2790-97.

Hong S, Kwon J, Kim DW, Lee HJ, Lee D, Mar W. Mulberrofuran G protects ischemic injury-induced cell death via inhibition of NOX4-mediated ROS generation and ER stress. Phytother Res. 2017; 31: 321-29.

Khan H, Singh RD, Tiwari R, Gangopadhyay S, Roy SK, Singh D, Srivastava V. Mercury exposure induces cytoskeleton disruption and loss of renal function through epigenetic modulation of MMP9 expression. Toxicology 2017; 386: 28-39.

Koirala P, Seong SH, Zhou Y, Shrestha S, Jung HA, Choi JS. Structure activity relationship of the tyrosinase inhibitors kuwanon G, mulberrofuran G, and albanol B from Morus Species: A kinetics and molecular docking study. Molecules (Basel, Switzerland). 2018; 23: 1413.

Li M, Wu X, Wang X, Shen T, Ren D. Two novel compounds from the root bark of *Morus alba* L. Nat Prod Res. 2018; 32: 36-42.

Li Y, Li Y, Zhang H, Shi R, Zhang Z, Liu H, Chen J. EML4-ALK-mediated activation of the JAK2-STAT pathway is critical for non-small cell lung cancer transformation. BMC Pulm Med. 2021; 21: 190.

Liang L, Hui K, Hu C, Wen Y, Yang S, Zhu P, Wang L, Xia Y, Qiao Y, Sun W, Fei J, Chen T, Zhao F, Yang B, Jiang X. Autophagy inhibition potentiates the anti-angiogenic property of multikinase inhibitor anlotinib through JAK2/STAT3/VEGFA signaling in non-small cell lung cancer cells. J Exp Clin Cancer Res. 2019; 38: 71.

Liang CC, Park AY, Guan JL. *In vitro* scratch assay: A convenient and inexpensive method for analysis of cell migration *in vitro*. Nat Protoc. 2007; 2: 329-33.

Liu R-Y, Zeng Y, Lei Z, Wang L, Yang H, Liu Z, Zhao J, Zhang H-T. JAK/STAT3 signaling is required for TGF-β-induced epithelial-mesenchymal transition in lung cancer cells. Int J Oncol. 2014; 44: 1643-51.

Liu X, Chen B, You W, Xue S, Qin H, Jiang H. The membrane bile acid receptor TGR5 drives cell growth and migration via activation of the JAK2/STAT3 signaling pathway in non-small cell lung cancer. Cancer Lett. 2018; 412: 194-207.

Mahmood T, Yang PC. Western blot: Technique, theory, and trouble shooting. North Am J Med Sci. 2012; 4: 429.

Niu G, Wright KL, Ma Y, Wright GM, Huang M, Irby R, Briggs J, Karras J, Cress WD, Pardoll D. Role of Stat3 in regulating p53 expression and function. Mol Cell Biol. 2005; 25: 7432-40.

Patel P, Tsiperson V, Gottesman SR, Somma J, Blain SW. Dual inhibition of CDK4 and CDK2 via targeting p27 tyrosine phosphorylation induces a potent and durable response in breast cancer cells. Mol Cancer Res. 2018; 16: 361-77.

Paudel P, Yu T, Seong SH, Kuk EB, Jung HA, Choi JS. Protein tyrosine phosphatase 1B inhibition and glucose uptake potentials of mulberrofuran G, albanol B, and kuwanon G from root bark of *Morus alba* L. in insulin-resistant HepG2 cells: An *in vitro* and *in silico* study. Int J Mol Sci. 2018; 19: 1542.

Pijuan J, Barceló C, Moreno DF, Maiques O, Sisó P, Marti RM, Macià A, Panosa A. *In vitro* cell migration, invasion, and adhesion assays: From cell imaging to data analysis. Front Cell Dev Biol. 2019; 7: 107.

Pyo JS, Kim HH, Kim KM, Kang JS. Amelioration of dry eye syndrome by oral administration of cultivated wild ginseng extract. Bangladesh J Pharmacol. 2019; 14: 61-66.

Ramalingam V, Revathidevi S, Shanmuganayagam T, Muthulakshmi L, Rajaram R. Gold nanoparticle induces mitochondria-mediated apoptosis and cell cycle arrest in non-small cell lung cancer cells. Gold Bull. 2017; 50: 177-89.

Shanmugasundaram K, Nayak BK, Friedrichs WE, Kaushik D, Rodriguez R, Block K. NOX4 functions as a mitochondrial energetic sensor coupling cancer metabolic reprogramming to drug resistance. Nat Commun. 2017; 8: 997.

Sherr CJ. D-type cyclins. Trends Biochem Sci. 1995; 20: 187-90.

Singh K, Dong Q, TimiriShanmugam PS, Koul S, Koul HK. Tetrandrine inhibits deregulated cell cycle in pancreatic cancer cells: Differential regulation of p21Cip1/Waf1, p27Kip1 and cyclin D1. Cancer Lett. 2018; 425: 164-73.

Sun D, Shen W, Zhang F, Fan H, Xu C, Li L, Tan J, Miao Y, Zhang H, Yang Y. α-Hederin inhibits interleukin 6-induced

epithelial-to-mesenchymal transition associated with disruption of JAK2/STAT3 signaling in colon cancer cells. Biomed Pharmacother. 2018; 101: 107-14.

Szydłowski M, Dębek S, Prochorec-Sobieszek M, Szołkowska M, Tomirotti AM, Juszczyński P, Szumera-Ciećkiewicz A. PIM kinases promote survival and immune escape in primary mediastinal large B-cell lymphoma through modulation of JAK-STAT and NF-κB activity. Am J Pathol. 2021; 191: 567-74.

Tang Y, Tong X, Li Y, Jiang G, Yu M, Chen Y, Dong S. JAK2/STAT3 pathway is involved in the protective effects of epidermal growth factor receptor activation against cerebral ischemia/reperfusion injury in rats. Neurosci Lett. 2018; 662: 219-26.

Vandooren J, Van den Steen PE, Opdenakker G. Biochemistry and molecular biology of gelatinase B or matrix metalloproteinase-9 (MMP-9): the next decade. Crit Rev Biochem Mol Biol. 2013; 48: 222-72.

Welte T, Zhang SS, Wang T, Zhang Z, Hesslein DG, Yin Z, Kano A, Iwamoto Y, Li E, Craft JE. STAT3 deletion during hematopoiesis causes Crohn's disease-like pathogenesis and lethality: A critical role of STAT3 in innate immunity. Proc Natl Acad Sci. 2003; 100: 1879-84.

Weng L, Zhang H, Li X, Zhan H, Chen F, Han L, Xu Y, Cao X. Ampelopsin attenuates lipopolysaccharide-induced inflammatory response through the inhibition of the NF-κB and JAK2/STAT3 signaling pathways in microglia. Int Immunopharmacol. 2017; 44: 1-8.

Zhang JF, Wang P, Yan YJ, Li Y, Guan MW, Yu JJ, Wang XD. IL-33 enhances glioma cell migration and invasion by upregulation of MMP2 and MMP9 via the ST2-NF-κB pathway. Oncol Reports. 2017; 38: 2033-42.

Zhang X, Yin P, Di D, Luo G, Zheng L, Wei J, Zhang J, Shi Y, Zhang J, Xu N. IL-6 regulates MMP-10 expression via JAK2/STAT3 signaling pathway in a human lung adenocarcinoma cell line. Anticancer Res. 2009; 29: 4497-501.

Zhang Y, Wang DC, Shi L, Zhu B, Min Z, Jin J. Genome analyses identify the genetic modification of lung cancer subtypes. Seminars in cancer biology. Elsevier, 2017, pp 20-30.

Author Info
Xiao-Yong Zhu (Principal contact)
e-mail: zhuxyzj@126.com